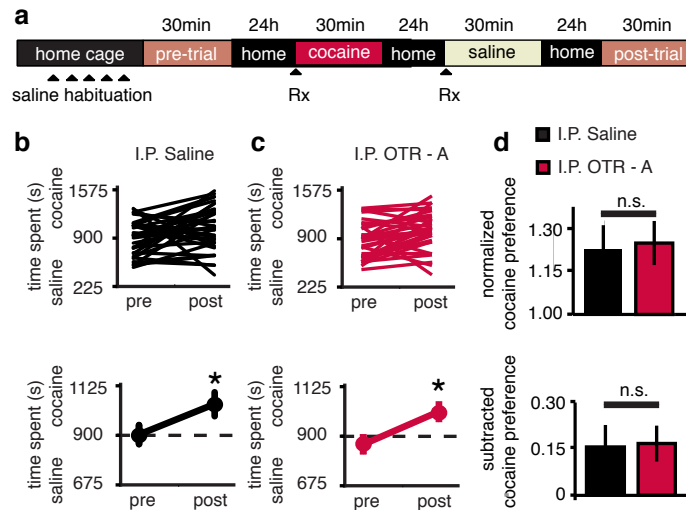
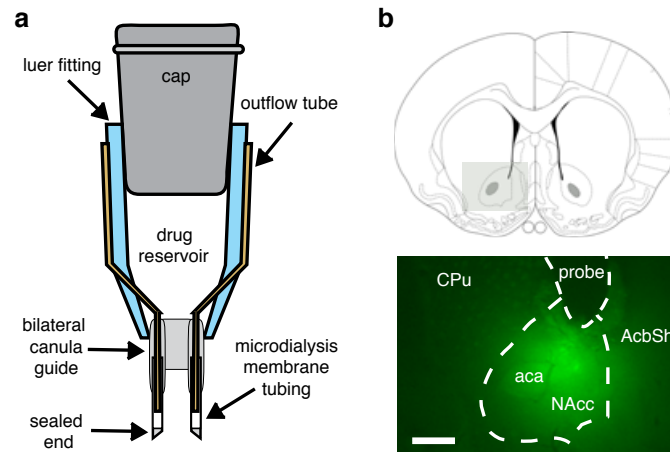


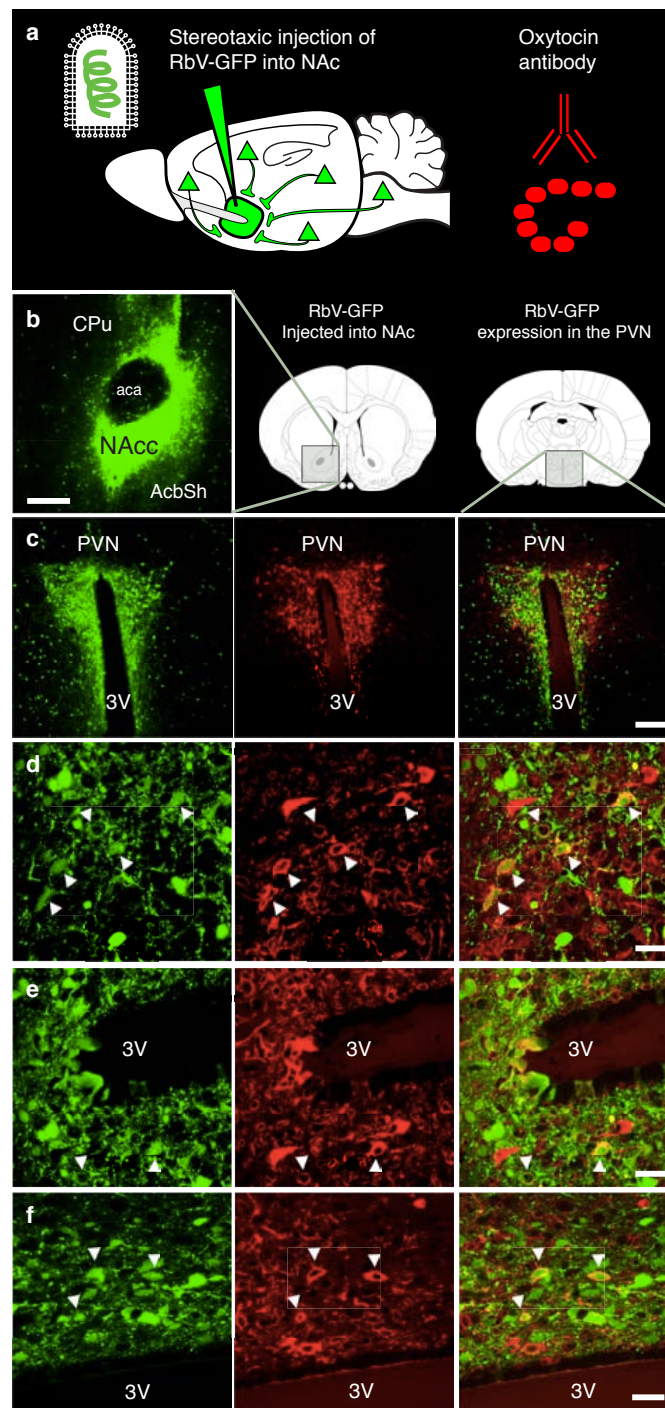
**Supplementary Figure 1. Locomotor activity is not altered by sCPP or OTR-A.** **a**, distance travelled is not different between groups (saline injected, pre  $3116 \pm 262$ , post  $2865 \pm 215$ ,  $n = 18$  animals,  $p = 0.450$ ; OTR-A injected, pre  $2862 \pm 179$ , post  $2936 \pm 354$ ,  $n = 15$  animals,  $p = 0.848$ ). **b**, ambulatory time is not different between groups (saline injected, pre  $92 \pm 7$ , post  $90 \pm 89$ ,  $n = 18$  animals,  $p = 0.830$ ; OTR-A injected, pre  $85 \pm 6$ , post  $89 \pm 9$ ,  $n = 15$  animals,  $p = 0.687$ ). **c**, ambulatory counts are not different between groups (saline injected, pre  $1421 \pm 184$ , post  $1330 \pm 142$ ,  $n = 18$  animals,  $p = 0.688$ ; OTR-A injected, pre  $1238 \pm 122$ , post  $1361 \pm 232$ ,  $n = 15$  animals,  $p = 0.630$ ). **d**, time stereotypic is not different between groups (saline injected, pre  $397 \pm 10$ , post  $383 \pm 15$ ,  $n = 18$  animals,  $p = 0.417$ ; OTR-A injected, pre  $402 \pm 6$ , post  $383 \pm 11$ ,  $n = 13$  animals,  $p = 0.111$ ). **e**, stereotypic counts are not different between groups (saline injected, pre  $5362 \pm 210$ , post  $5226 \pm 275$ ,  $n = 18$  animals,  $p = 0.689$ ; OTR-A injected, pre  $5453 \pm 141$ , post  $5133 \pm 192$ ,  $n = 13$  animals,  $p = 0.174$ ). **f**, resting time is not different between groups (saline injected, pre  $1308 \pm 14$ , post  $1284 \pm 36$ ,  $n = 18$  animals,  $p = 0.532$ ; OTR-A injected, pre  $1307 \pm 12$ , post  $1326 \pm 18$ ,  $n = 15$  animals,  $p = 0.368$ ). **g**, vertical counts are not different between groups (saline injected, pre  $220 \pm 18$ , post  $200 \pm 22$ ,  $n = 18$  animals,  $p = 0.466$ ; OTR-A injected, pre  $217 \pm 20$ , post  $197 \pm 38$ ,  $n = 11$  animals,  $p = 0.628$ ). **h**, vertical time is not different between groups (saline injected, pre  $138 \pm 11$ , post  $123 \pm 11$ ,  $n = 18$  animals,  $p = 0.346$ ; OTR-A injected, pre  $145 \pm 13$ , post  $127 \pm 17$ ,  $n = 11$  animals,  $p = 0.384$ ). **i**, number of transitions are not different between groups (saline injected, pre  $85 \pm 7$ , post  $74 \pm 8$ ,  $n = 18$  animals,  $p = 0.306$ ; OTR-A injected, pre  $81 \pm 12$ , post  $87 \pm 19$ ,  $n = 15$  animals,  $p = 0.759$ ). Summary data are presented as mean  $\pm$  s.e.m. (\* $P < 0.05$ ).



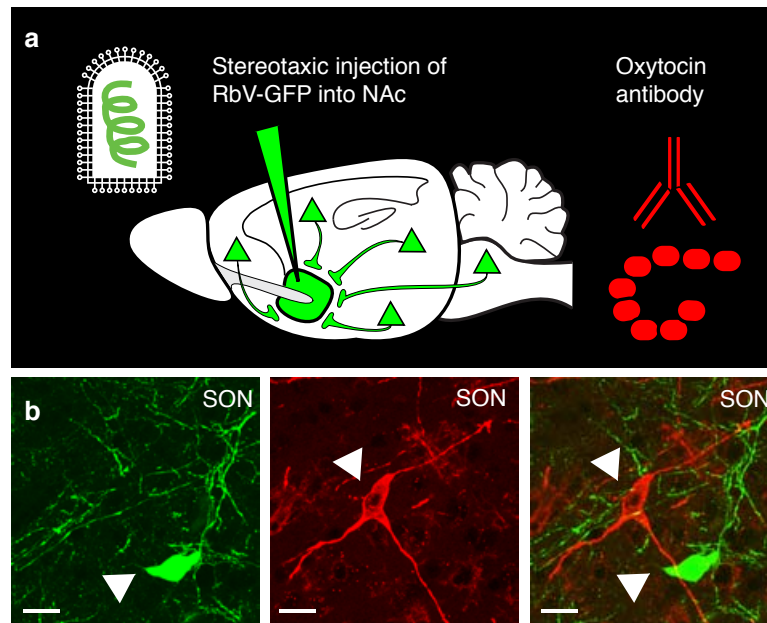
**Supplementary Figure 2. Cocaine conditioned place preference (cCPP) does not require OT.** **a**, Experimental time course for cocaine CPP. **b-c**, Individual (top) and average (bottom) responses in i.p. saline injected (**b**), versus i.p. OTR-A injected (**c**) animals. Both i.p. saline and i.p. OTR-A injected animals, spend more time in the cocaine context following conditioning (i.p. saline, pre  $903 \pm 43$ , post  $1042 \pm 54$ ,  $n = 34$  animals,  $p = 0.034$  paired t-test; i.p. OTR-A, pre  $863 \pm 46$ , post  $1011 \pm 47$ ,  $n = 32$  animals,  $p = 0.007$  paired t-test). **d**, Comparisons between i.p. saline versus i.p. OTR-A treated animals reveals no difference in normalized cocaine preference and subtracted cocaine preference in OTR-A treated animals (normalized saline  $1.225 \pm 0.079$ , OTR-A  $1.245 \pm 0.074$ ,  $p = 0.906$  unpaired t-test; subtracted saline  $0.154 \pm 0.069$ , OTR-A  $0.165 \pm 0.057$ ,  $p = 0.857$  unpaired t-test). Summary data are presented as mean  $\pm$  s.e.m (\* $P < 0.05$ ).



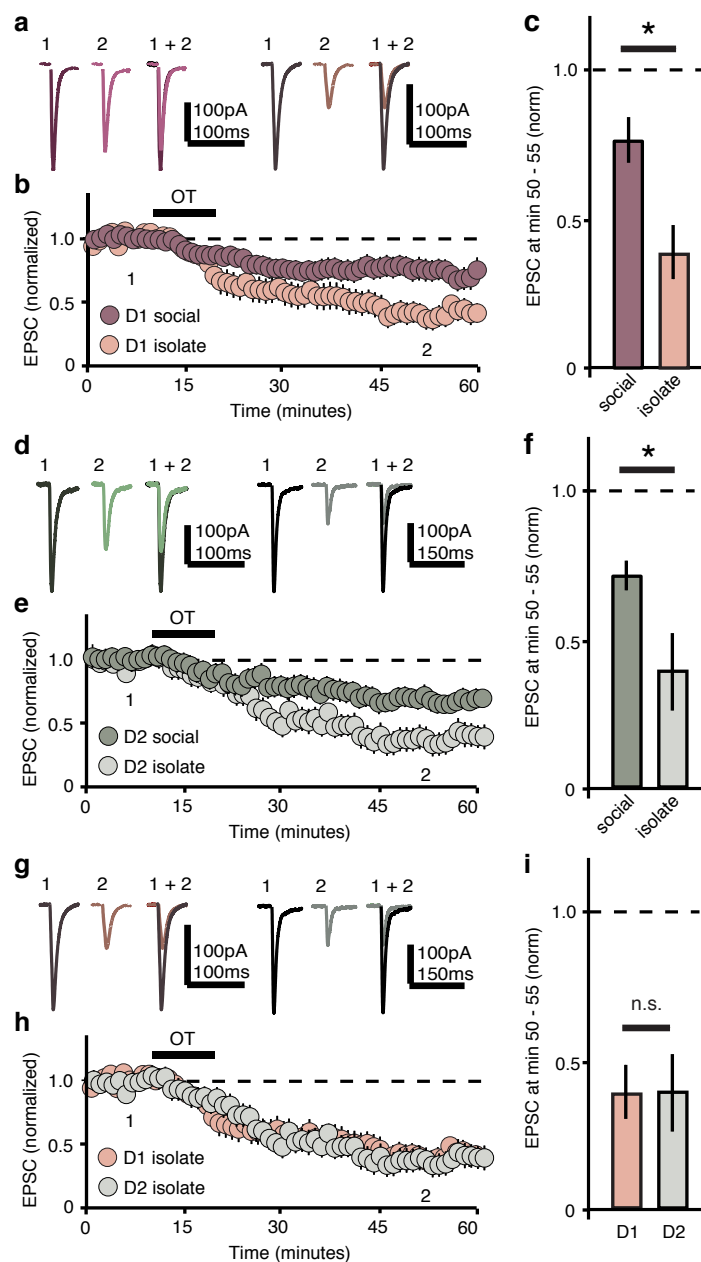
**Supplementary Figure 3. Andalman reverse microdialysis probes. a,** Schematic of Andalman probe for reverse microdialysis experiments in Fig. 1f-i and 5l-o. **b,** Post-hoc confirmation of probe placement and competency.



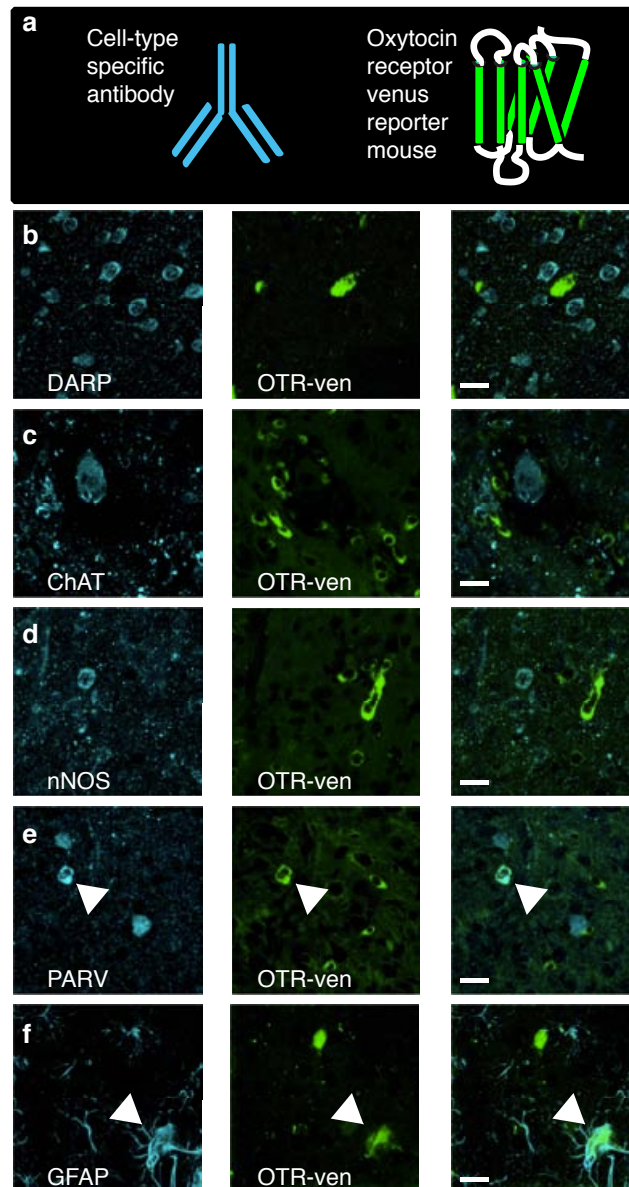
**Supplementary Figure 4. OT expressing neurons in the paraventricular nucleus (PVN) send projections to the NAc.** **a**, Diagram illustrating the injection of RbV-GFP into the NAc, followed by antibody labeling of OT producing neurons in the PVN. **b**, Localization and expression of RbV-GFP in the NAc (scale bars 200  $\mu$ m). **c-f**, Low magnification (**c**, scale bar 100  $\mu$ m) and high magnification (**d-f**, scale bars 20  $\mu$ m) images of PVN cells that have been retrogradely labeled by RbV-GFP taken up by presynaptic terminals in the NAc (green, left panels) and labeled by ant-OT-np antibody (red, center panels). Co-localization (merged right panels) indicates oxytocinergic neurons that project to the NAc; arrowheads highlight individual cells that show co-localization. (Nucleus accumbens core, NAcc; nucleus accumbens shell, AcbSh; anterior commissure, aca; caudate putamen, CPu; third ventricle, 3V; paraventricular nucleus of the hypothalamus, PVN)



**Supplementary Figure 5. OT expressing neurons in the Supraoptic Nucleus (SON) do not send projections to the NAc.** **a**, Diagram illustrating the injection of RbV-GFP into the NAc, followed by antibody labeling of OT producing neurons in the SON. **b**, high magnification (scale bars 20  $\mu$ m) images of SON cells that have been retrogradely labeled by RbV-GFP taken up by presynaptic terminals in the NAc (green, left panels) or labeled by ant-OT-np antibody (red, center panels). Absence of co-localization (merged right panels) indicates oxytocinergic neurons do not project to the NAc.

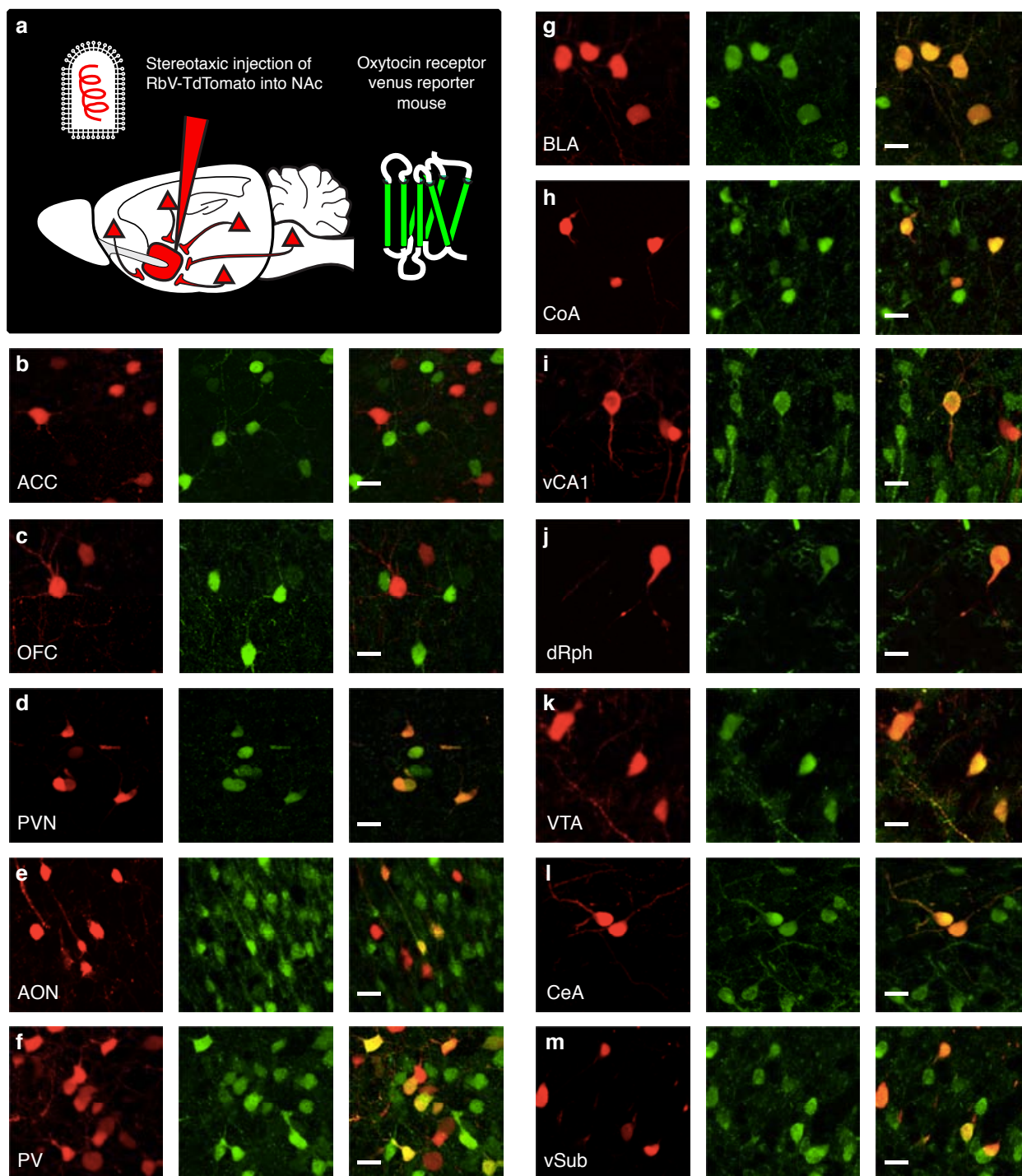


**Supplementary Figure 6. Increased magnitude of OT-LTD in both D1 and D2 receptor expressing MSN following isolation conditioning.** **a-h**, Representative traces (**a,d,g**), summary time course (**b,e,h**), and average post-treatment magnitude comparisons (**c,f,i**) reveal that the magnitude of OT-LTD is significantly increased in both D1 (**a-c**) and D2 (**d-f**) cells from isolation versus socially reared animals (D1 isolation,  $0.379 \pm 0.090$ ,  $n = 6$  cells and D1 social,  $0.756 \pm 0.078$ ,  $n = 9$  cells,  $p = 0.00524$  unpaired t-test; D2 isolation,  $0.386 \pm 0.129$ ,  $n = 5$  and D2 social,  $0.708 \pm 0.051$ ,  $n = 11$  cells,  $p = 0.00845$  unpaired t-test); and the magnitude of EPSC OT-LTD is not different in D1 versus D2 MSNs from slices made from isolation conditioned animals (**g-i**) ( $p = 0.957$  unpaired t-test). Representative traces are binned from 5 consecutive sweeps taken at times indicated (1 and 2). Summary data are presented as mean  $\pm$  s.e.m (\* $P < 0.05$ ).



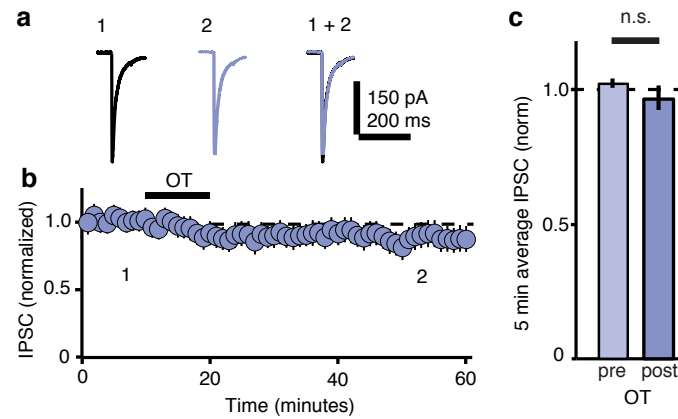
**Supplementary Figure 7. OT receptor (OTR) expressing cells in the NAc.** **a**, Diagram illustrating immunolabeling with cell-type specific antibodies in the NAc of OTR-Venus mice. **b**, DARP positive MSNs (blue, left) and OTR-Ven positive cells (green, center) do not co-localize (merge, right). **c**, CHAT positive cholinergic interneurons (blue, left) and OTR-Ven positive cells (green, center) do not co-localize (merge, right). **d**, nNOS positive inhibitory interneurons (blue, left) and OTR-Ven positive cells (green, center) do not co-localize (merge, right). **e**, a subset of PARV positive inhibitory interneurons (blue, left) and OTR-Venus positive cells (green, center) show co-localization (merge, right). **f**, a subset of GFAP positive glial cells (blue, left) and OTR-Ven positive cells (green, center) show co-localization (merge, right). (Scale bars 20  $\mu$ m)



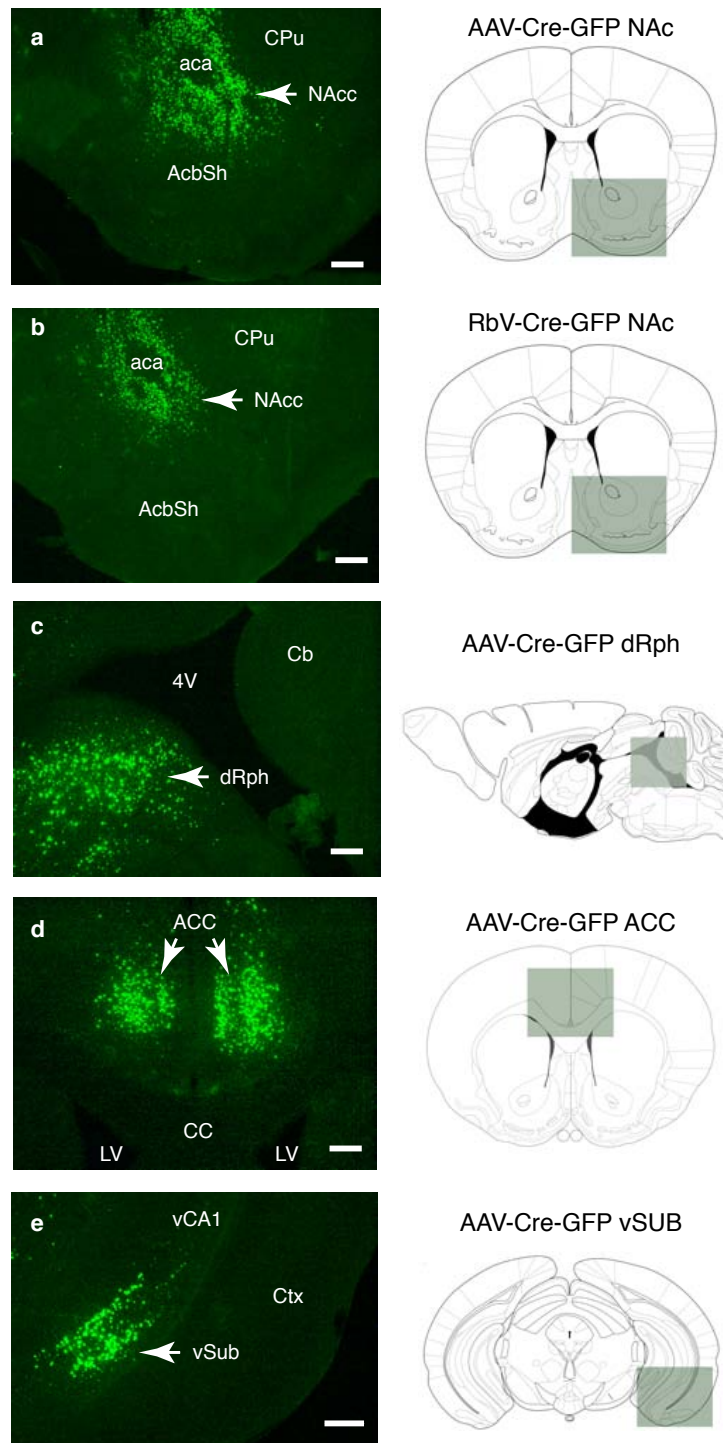


**Supplementary Figure 8. OT receptor expressing cells that project to the NAc.** **a**, Diagram illustrating stereotaxic injection of RbV-TdTomato into the NAc of OTR-Venus mice. **b-m**, high magnification images of cells in the (b) anterior cingulate cortex, ACC; (c) orbitofrontal cortex, OFC; (d) paraventricular nucleus of the hypothalamus, PVN; (e) anterior olfactory nucleus, AON; (f) paraventricular thalamus, PV; (g) basolateral amygdala, BLA; (h) cortex of the amygdala, CoA; (i) ventral hippocampal CA1, vCA1; (j) dorsal Raphe nucleus, dRph; (k) caudal ventral tegmental nucleus, VTA; (l) central amygdala, CeA; and ventral subiculum, vSub that have been retrogradely labeled by RbV-GFP taken up by presynaptic terminals in the NAc (red, left panels) and that express OTR-Venus (green, center panels). Co-localization (merge, right panels) is notably absent in (b) ACC and (c) OFC, but in all other regions (d-m), a subset of cells show clear co-localization (project to the NAc and express OTR-Venus), implicating these neurons as a putative source of presynaptic OTRs in the NAc. (Scale bars 20  $\mu$ m).

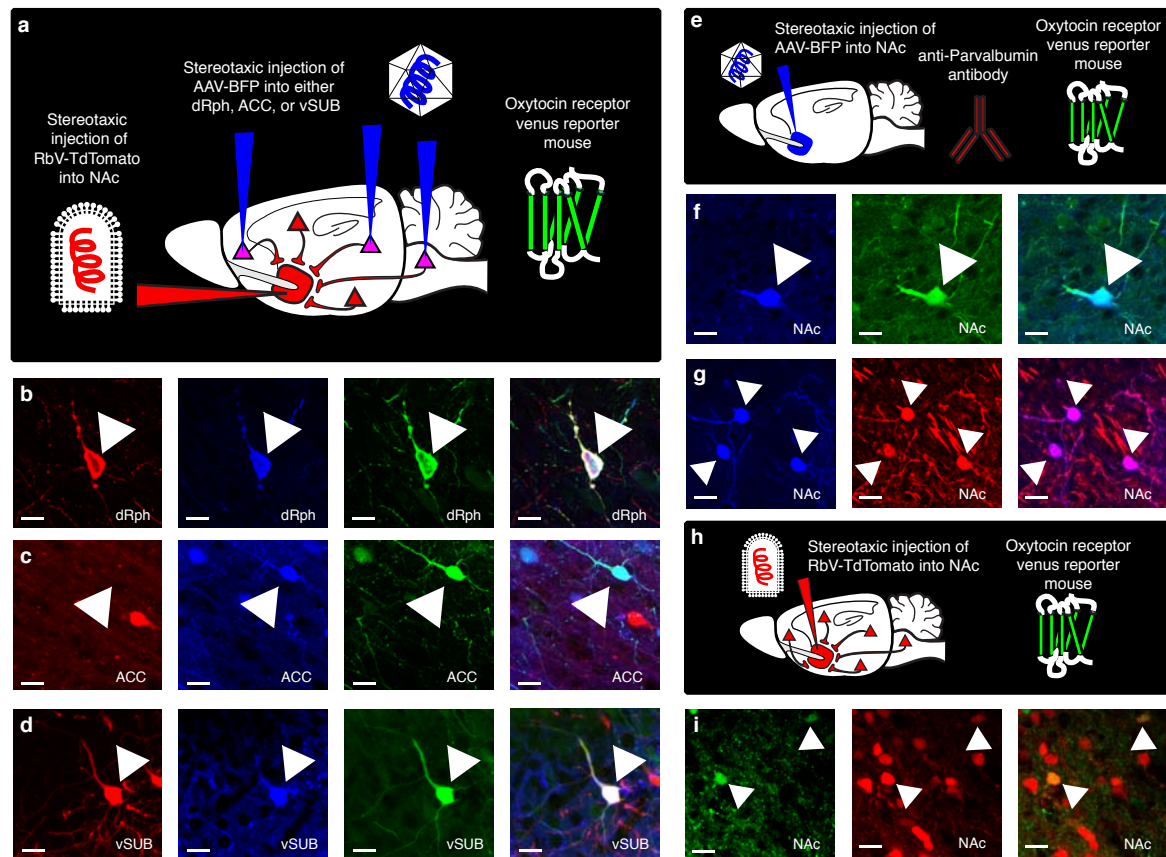




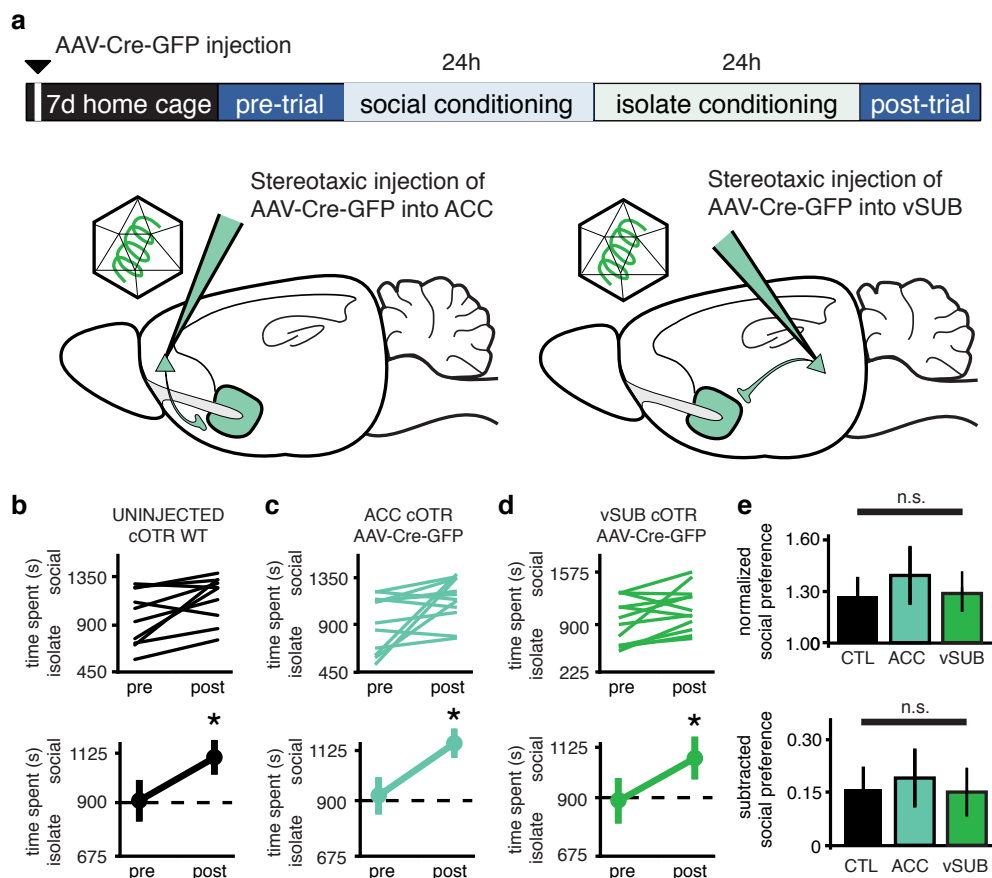
**Supplementary Figure 9. OT does not alter inhibitory postsynaptic currents (IPSCs) recorded from NAc MSNs.** Representative traces (a), summary time course (b) and average post-treatment magnitude comparisons (c) reveal absence of significant OT-induced changes in IPSC amplitude (pre  $1.023 \pm 0.0186$ , post  $0.962 \pm 0.0456$ ,  $n = 11$  cells,  $p = 0.557$  paired t-test). Representative traces are binned from 5 consecutive sweeps taken at times indicated (1 and 2). Summary data are presented as mean  $\pm$  s.e.m ( $*P < 0.05$ ).



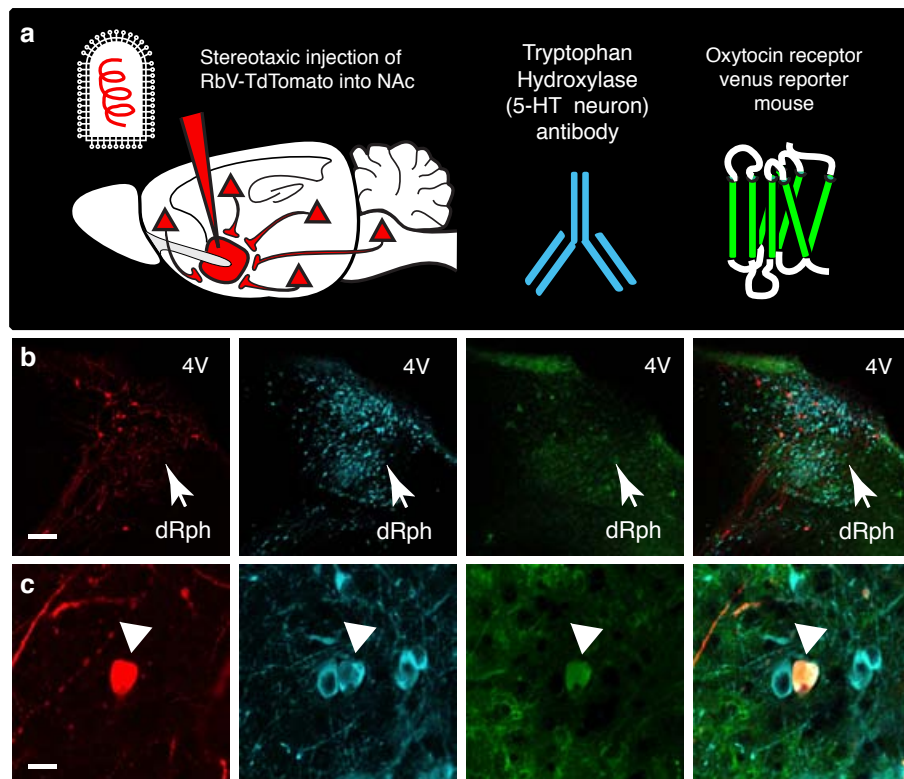
**Supplementary Figure 10. Post-hoc confirmation of viral injection sites and transgene expression.** **a,b** Localization and expression of (a) AAV-Cre-GFP and (b) RbV-Cre-GFP stereotaxic injections into the NAc. **c,d,e**, Localization and expression of AAV-Cre-GFP stereotaxic injections into the (c) dRph, (d) ACC and (e) vSub. (Nucleus accumbens core, NAcc; nucleus accumbens shell, AcbSh; anterior commissure, aca; caudate putamen a.k.a. dorsal striatum, CPu; dorsal Raphe, dRph; fourth ventricle, 4V; cerebellum, Cb; anterior cingulate cortex, ACC; corpus callosum, CC; lateral ventricle, LV; ventral subiculum, vSub; ventral CA1 region of the hippocampus, vCA1; entorhinal cortex, Ctx; Scale bars 250  $\mu$ m)



**Supplementary Figure 11. Confirmation of viral tropism for OTR-expressing and NAc-projecting cells.** **a**, Diagram illustrating stereotaxic injection of RbV-TdTomato into the NAc of OTR-Venus mice followed by AAV-BFP expression in either dorsal Raphe nucleus, dRph, anterior cingulate cortex, ACC or ventral subiculum, vSub shown in (**b-d**). **b-d**, high magnification images of cells in the (b) dRph (c) ACC or (d) vSub that have been retrogradely labeled by RbV-GFP taken up by presynaptic terminals in the NAc (red, left panels), labeled by local infection with AAV-BFP (blue, center left), and that express OTR-Venus (green, center right panels). Clear co-localization (merge, right panels) between RbV-TdTomato, OTR-Venus and AAV-BFP is evident in (b and d) and co-localization between OTR-Venus and AAV-BFP is evident (c). **e**, Diagram illustrating stereotaxic injection of AAV-BFP into the NAc of OTR-Venus mice or WT mice followed by subsequent immunohistochemistry with anti-Parvalbumin antibody shown in (**f-g**). **f**, Local infection with AAV-BFP (blue, left) in cells that express OTR-Venus (green, center). Co-localization (merge, right) indicates AAV tropism for OTR expressing cells in the NAc. **g**, Local infection with AAV-BFP (blue, left) in cells that express Parvalbumin (red, center). Co-localization (merge, right) indicates AAV tropism for Parvalbumin expressing cells in the NAc. **h**, Diagram illustrating stereotaxic injection of RbV-TdTomato into the NAc of OTR-Venus mice shown in (i). **i**, Local infection with RbV-TdTomato (red, left) in cells that express OTR-Venus (green, center). Co-localization (merge, right) indicates RbV tropism for OTR expressing cells in the NAc. (Scale bars 20  $\mu$ m).

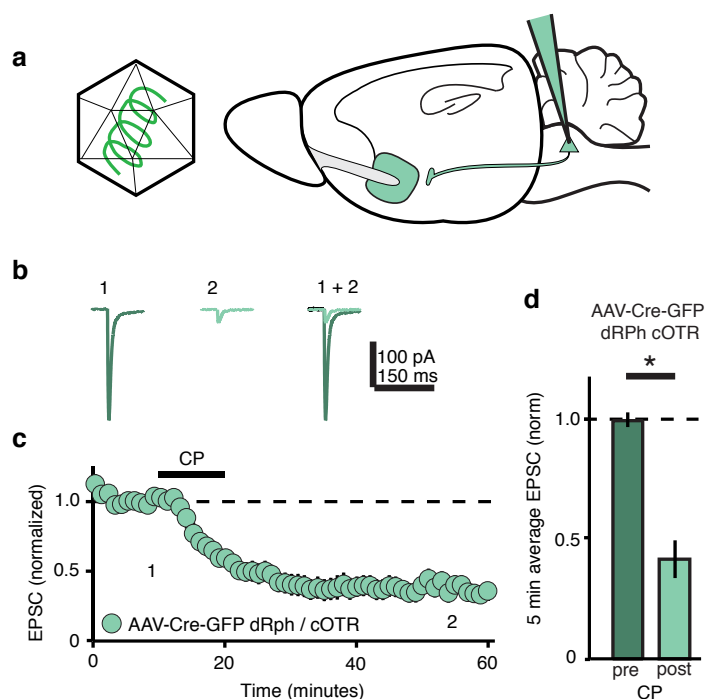


**Supplementary Figure 12. ACC and vSub OT receptors (OTRs) are not required for sCPP.** **a**, Diagram illustrating time course of viral injections into the ACC and vSub for sCPP experiments in **b-e**. **b,c,d** Individual (top) and average (bottom) preference scores indicate that un-injected cOTR KO animals (**b**), cOTR KO animals injected with AAV-Cre-GFP into the ACC (**c**) and cOTR KO animals injected with AAV-Cre-GFP into the vSub (**d**) have increased preference for the social bedding cue after conditioning (un-injected cOTR KO, pre  $935 \pm 82$ , post  $1151 \pm 68$ ,  $n = 10$ ,  $p = 0.044$  paired t-test; cOTR KO AAV-Cre-GFP ACC, pre  $935 \pm 78$ , post  $1160 \pm 61$ ,  $n = 12$ ,  $p = 0.034$ ; cOTR KO AAV-Cre-GFP vSub, pre  $907 \pm 90$ , post  $1085 \pm 85$ ,  $n = 12$ ,  $p = 0.043$ ). **e**, Comparisons between un-injected cOTR KO versus cOTR KO animals injected with AAV-Cre-GFP into the ACC or vSub reveals no difference in normalized social preference and subtracted social preference (normalized uninjected  $1.250 \pm 0.095$ , cOTR KO AAV-Cre-GFP ACC  $1.362 \pm 0.166$ , cOTR KO AAV-Cre-GFP vSub  $1.271 \pm 0.124$ ,  $p = 0.812$ , ANOVA; subtracted uninjected  $0.212 \pm 0.078$ , cOTR KO AAV-Cre-GFP ACC  $0.251 \pm 0.104$ , cOTR KO AAV-Cre-GFP vSub  $0.199 \pm 0.087$ ,  $p = 0.912$ , ANOVA). Summary data are presented as mean  $\pm$  s.e.m. (\* $P < 0.05$ ).

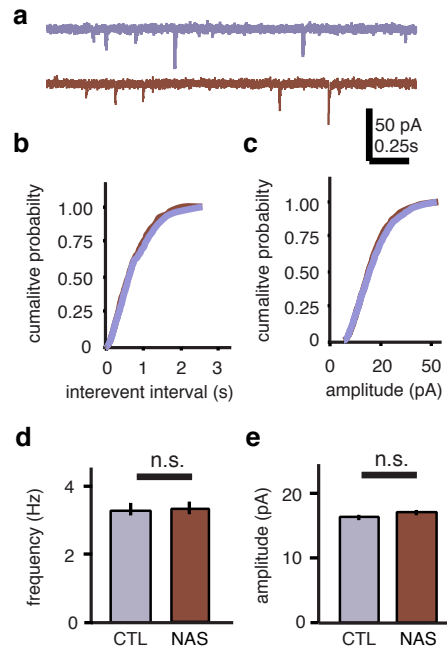


**Supplementary Figure 13. OT receptor-expressing cells in the dRph send serotonergic projections to the NAc.** **a**, Diagram illustrating stereotaxic injection of RbV-TdTomato into the NAc of OTR-Venus reporter mice, followed by subsequent immunohistochemistry with anti-tryptophan hydroxylase antibodies to label serotonergic neurons of the dRph. **b,c**, Low magnification (**b**, scale bar 200  $\mu$ m) and high magnification (**c**, scale bar 20  $\mu$ m) images of neurons in the dRph that send projections to the NAc (red, left), express OTR (green, middle left) and produce 5-HT (blue, middle right). Arrowheads and merged image (right) shows subset of neurons that show colocalization. (dorsal raphe, dRph; fourth ventricle, 4V).

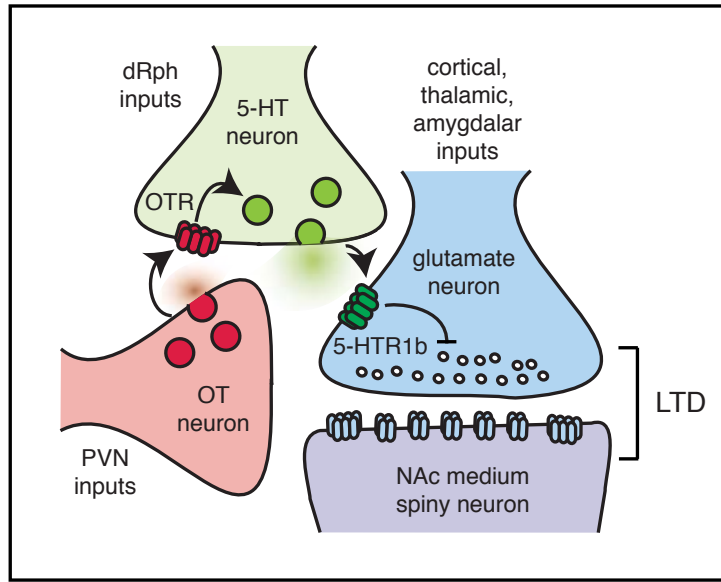




**Supplementary Figure 14. Molecular ablation of OTRs in dorsal raphe does not disrupt 5HT1b agonist induced LTD.** **a**, Diagram illustrating time course of viral injections into the dRph for LTD experiments in **b-d**. Representative traces (**b**), summary time course (**c**) and average post-treatment magnitude comparisons (**d**) reveal 5HT1b induced-LTD in EPSCs recorded from cOTR animals whose OTRs had been molecularly ablated by AAV-Cre-eGFP dRph injection (dRph-AAV-Cre-eGFP injected cOTR, pre  $1.0158 \pm 0.0315$ , post  $0.3566 \pm 0.0891$ ,  $n = 5$  cells,  $p = 0.0031$  paired t-test). Representative traces are binned from 5 consecutive sweeps taken at times indicated (1 and 2). Summary data are presented as mean  $\pm$  s.e.m (\* $P < 0.05$ ).



**Supplementary Figure 15. 5HTR1b-A alone does not alter mini EPSC frequency or amplitude.** **a**, Representative miniature EPSCs (mEPSCs) recorded in control neurons (purple) and neurons treated with NAS-181 (red, 20  $\mu$ M, 10 minutes). **b**, Cumulative probability (top) and average (bottom) mEPSC frequency is not decreased in NAS-treated cells compared to control cells (control  $3.31 \pm 0.456$ ,  $n = 10$  cells, NAS-181  $3.36 \pm 0.409$ ,  $n = 10$  cells;  $p = 0.9346$  unpaired t-test). **c**, Cumulative probability (top) and average (bottom) mEPSC amplitude is not different in NAS-treated cells compared to control cells (control  $16.13 \pm 1.152$ ,  $n = 10$  cells, NAS-181  $16.90 \pm 0.886$ ,  $n = 10$  cells;  $p = 0.5826$  unpaired t-test). Summary data are presented as mean  $\pm$  s.e.m (\* $P < 0.05$ ).



**Supplementary Figure 16. Diagram illustrating model for induction of OT-induced LTD in NAc.** OT producing neurons from the PVN release OT into the NAc. Activation of OTRs on presynaptic terminals of 5-HT neurons from the dRph causes the release of 5-HT into the NAc. Activation of 5HT1b receptors on glutamatergic terminals from various brain regions (cortex, amygdala, thalamus) decrease presynaptic function at excitatory synapses onto MSNs.